



## Biochemical characterization of recombinant *guaA*-encoded guanosine monophosphate synthetase (EC 6.3.5.2) from *Mycobacterium tuberculosis* H37Rv strain

Tathiana Mar A. Franco<sup>a,b</sup>, Diana C. Rostirolla<sup>a,b</sup>, Rodrigo G. Ducati<sup>a</sup>, Daniel M. Lorenzini<sup>a</sup>, Luiz A. Basso<sup>a,b,\*</sup>, Diógenes S. Santos<sup>a,b,\*</sup>

<sup>a</sup> Instituto Nacional de Ciência e Tecnologia em Tuberculose (INCT-TB), Centro de Pesquisas em Biologia Molecular e Funcional (CPBMF), Pontifícia Universidade Católica do Rio Grande do Sul (PUCRS), Av. Ipiranga 6681/Prédio 92-A, 90619-900 Porto Alegre, RS, Brazil

<sup>b</sup> Programa de Pós-Graduação em Medicina e Ciências da Saúde, PUCRS, Porto Alegre, RS, Brazil

### ARTICLE INFO

#### Article history:

Received 7 July 2011

and in revised form 8 November 2011

Available online 18 November 2011

#### Keywords:

Guanosine monophosphate synthetase  
Recombinant protein  
Steady-state kinetics  
Cooperative kinetics  
Protein function  
Tuberculosis

### ABSTRACT

Administration of the current tuberculosis (TB) vaccine to newborns is not a reliable route for preventing TB in adults. The conversion of XMP to GMP is catalyzed by *guaA*-encoded GMP synthetase (GMPS), and deletions in the *Shigella flexneri* *guaBA* operon led to an attenuated auxotrophic strain. Here we present the cloning, expression, and purification of recombinant *guaA*-encoded GMPS from *Mycobacterium tuberculosis* (MtGMPS). Mass spectrometry data, oligomeric state determination, steady-state kinetics, isothermal titration calorimetry (ITC), and multiple sequence alignment are also presented. The homodimeric MtGMPS catalyzes the conversion of XMP, MgATP, and glutamine into GMP, ADP, PP<sub>i</sub>, and glutamate. XMP, NH<sub>4</sub><sup>+</sup>, and Mg<sup>2+</sup> displayed positive homotropic cooperativity, whereas ATP and glutamine displayed hyperbolic saturation curves. The activity of ATP pyrophosphatase domain is independent of glutamine amidotransferase domain, whereas the latter cannot catalyze hydrolysis of glutamine to NH<sub>3</sub> and glutamate in the absence of substrates. ITC data suggest random order of binding of substrates, and PP<sub>i</sub> is the last product released. Sequence comparison analysis showed conservation of both Cys-His-Glu catalytic triad of N-terminal Class I amidotransferase and of amino acid residues of the P-loop of the N-type ATP pyrophosphatase family.

© 2011 Elsevier Inc. All rights reserved.

### Introduction

Human tuberculosis (TB) remains a major global health concern worldwide. In 1993, the World Health Organization (WHO<sup>1</sup>) de-

\* Corresponding authors at: Instituto Nacional de Ciência e Tecnologia em Tuberculose (INCT-TB), Centro de Pesquisas em Biologia Molecular e Funcional (CPBMF), Pontifícia Universidade Católica do Rio Grande do Sul (PUCRS), Av. Ipiranga 6681/Prédio 92-A, 90619-900 Porto Alegre, RS, Brazil. Fax: +55 51 33203629.

E-mail addresses: [luiz.basso@pucrs.br](mailto:luiz.basso@pucrs.br) (L.A. Basso), [diogenes@pucrs.br](mailto:diogenes@pucrs.br) (D.S. Santos).

<sup>1</sup> Abbreviations used: AMP, adenosine 5'-monophosphate; ATP, adenosine 5'-triphosphate; ATPase, ATP pyrophosphatase; BCG, bacille Calmette-Guérin; DMSO, dimethyl sulfoxide; GATase, glutamine amidotransferase; GMP, guanosine 5'-monophosphate; GMPS, guanosine monophosphate synthetase; Hepes, N-2-hydroxyethylpiperazine-N'-2-ethanesulfonic acid; IMP, inosine 5'-monophosphate; IMPDH, inosine monophosphate dehydrogenase; IPTG, isopropyl-β-D-thiogalactopyranoside; ITC, isothermal titration calorimetry; LB, Luria-Bertani; MDR, multidrug-resistant; MESG, 2-amino-6-mercapto-7-methylpurine ribonucleoside; MtGMPS, *M. tuberculosis* GMPS; P<sub>i</sub>, inorganic phosphate; PNP, purine nucleoside phosphorylase; PP<sub>i</sub>, pyrophosphate; SDS-PAGE, sodium dodecyl sulfate-polyacrylamide gel electrophoresis; TB, tuberculosis; TDR, totally drug-resistant; Tris, tris(hydroxymethyl)aminomethane; WHO, World Health Organization; XDR, extensively drug-resistant; XMP, xanthosine 5'-monophosphate.

clared TB as a global health emergency. Recent epidemiological studies have shown that each year up to 9.4 million people are infected with *Mycobacterium tuberculosis*, the main aetiological agent of TB, causing approximately 3 million deaths [1]. The efficacy of TB chemotherapy has been diminished due to the emergence of multidrug-resistant (MDR), extensively drug-resistant (XDR) [2], and totally drug-resistant (TDR) [3] strains. The global burden of TB remains high, particularly in countries with high prevalence of drug-resistance and TB-HIV co-infection [4]. Despite important achievements, the control of TB epidemic remains elusive, which underlines the need for new strategies to combat TB.

Although the only vaccine currently in use, bacille Calmette-Guérin (BCG), protects very young children from invasive forms of TB, adolescents and adults are variably protected and remain susceptible to pulmonary diseases caused by *M. tuberculosis* [5]. The synthesis of guanosine 5'-monophosphate (GMP) from inosine 5'-monophosphate (IMP) requires both *guaB*-encoded inosine monophosphate dehydrogenase (IMPDH) and *guaA*-encoded guanosine monophosphate synthetase (GMPS). Deletions in the *Shigella flexneri* *guaBA* operon led to an attenuated auxotrophic strain that conferred both immunogenicity and safety in volunteers

[6,7]. As *Francisella tularensis* [8] and unlike enteric organisms, the *M. tuberculosis* H37Rv *guaB* and *guaA* genes are not located in a bicistronic operon, but rather present as independent *loci* [9]. Of the three IMPDH paralogs in *M. tuberculosis* (*guaB1*, Rv1843c; *guaB2*, Rv3411c; and *guaB3*, Rv3410c), *guaB2* has been shown to encode a protein with IMPDH activity that was tested as target for triazole-linked enzyme inhibitors [10].

GMPS (EC 6.3.5.2) is a key enzyme in both purine *de novo* synthesis and salvage pathways [11,12] of guanine nucleotides, and belongs to a G-type amidotransferase family that catalyzes the conversion of xanthosine 5'-monophosphate (XMP) and L-glutamine in the presence of H<sub>2</sub>O, adenosine 5'-triphosphate (ATP), and Mg<sup>2+</sup> into GMP, pyrophosphate (PP<sub>i</sub>), adenosine 5'-monophosphate (AMP), and L-glutamate (Fig. 1) [13,14]. In both prokaryotes and eukaryotes, the tertiary structure of GMPS is formed by two domains with distinct functions. The C-terminal ATP pyrophosphatase (ATPPase) domain catalyzes the condensation of XMP with ATP, and the N-terminal glutamine amidotransferase (glutaminase; GATase) domain catalyzes the hydrolysis of glutamine to ammonia and glutamate [15]. Biochemical studies have been reported for GMPS enzymes from human [13], *Escherichia coli* [16], *F. tularensis* [8], *Pyrococcus horikoshii* [17], and *Plasmodium falciparum* [15]. The *guaA*-encoded protein has been predicted to be essential for *in vitro* growth of *M. tuberculosis* based on transposon-site hybridization studies [18]. However, no formal biochemical data have been presented to show whether or not the *guaA* gene codes for a protein with GMPS activity as predicted by *in silico* analysis of *M. tuberculosis* genome sequence. To pave the way for further efforts to show that deletion of the *guaA* gene may result in an auxotrophic *M. tuberculosis* strain for guanine with attenuated virulence, biochemical characterization of the *guaA*-encoded protein is worth pursuing. Accordingly, here we describe the cloning, expression, purification to homogeneity, mass spectrometry, oligomeric state determination, steady-state kinetics, isothermal titration calorimetry (ITC), and multiple sequence alignment of *M. tuberculosis* GMPS (MtGMPS). It is hoped that these data may contribute to functional efforts towards a better understanding of the basic biology of *M. tuberculosis*.

## Materials and methods

### PCR amplification, cloning, and recombinant protein expression

Synthetic oligonucleotide primers (5'-tgcatatggtgcagcctgctgacatcgacg-3' and 5'-ggggatcctcactcccactcgatggtggc-3') complementary to the amino-terminal coding and carboxy-terminal noncoding strands of the *M. tuberculosis* *guaA* (Rv3396c) gene [9] were designed to contain, respectively, *Nde*I and *Bam*HI restriction sites (in bold). These primers were used to amplify the *guaA* structural gene (1578 bp) from *M. tuberculosis* H37Rv genomic DNA using standard PCR conditions (Perkin-Elmer), in the presence of 5% dimethyl sulfoxide (DMSO; final concentration). The PCR

product was digested with *Nde*I and *Bam*HI (New England Biolabs), and ligated into a pET23a(+) expression vector (Novagen). The DNA sequence of the cloned fragment, expected to correspond to the *M. tuberculosis* *guaA* gene, was determined by automated DNA sequencing to confirm gene identity and integrity, and ensure that no mutations were introduced by the PCR amplification step.

The recombinant pET23a(+):*guaA* plasmid was introduced into *E. coli* BL21(DE3) (Novagen) electrocompetent host cells by electroporation, and the transformed cells were selected on Luria-Bertani (LB) agar plates containing 50 µg mL<sup>-1</sup> ampicillin. LB medium (2.5 L) containing 50 µg mL<sup>-1</sup> ampicillin was inoculated with single colonies, and the bacterial culture grown at 180 rpm and 37 °C for 6 h after reaching an OD<sub>600nm</sub> = 0.4–0.6, without isopropyl-β-D-thiogalactopyranoside (IPTG) induction. Cells were harvested by centrifugation at 4,000g for 30 min at 4 °C and stored at –20 °C. Soluble and insoluble fractions were analyzed by 12% sodium dodecyl sulfate–polyacrylamide gel electrophoresis (SDS–PAGE) [19].

### Protein purification

All purification steps were performed using an Äkta Purifier (GE Healthcare) system at 4 °C. Approximately 2 g of wet cell paste were suspended in 10 mL of 50 mM tris(Hydroxymethyl)amino-methane (Tris) pH 7.5 (buffer A) and gently stirred for 30 min in the presence of 0.2 mg mL<sup>-1</sup> lysozyme (Sigma Aldrich; final concentration). Cells were disrupted by sonication with 10 pulses of 10 s each at 60% amplitude with a 13 mm probe, and cell debris was removed by centrifugation at 48,000g for 30 min. To precipitate nucleic acids and ribonuclear proteins, the supernatant was treated with 1% (wt./vol.) streptomycin sulfate (final concentration) for 30 min and centrifuged at 48,000g for 30 min. The supernatant was dialyzed against buffer A and loaded on a Q-Sepharose Fast Flow (GE Healthcare) anion exchange column, pre-equilibrated with buffer A. Adsorbed protein elution was carried out using a 0–0.4 M NaCl linear gradient in buffer A, and the fractions containing the target protein were pooled, concentrated using an Amicon ultrafiltration membrane (10 kDa molecular weight cutoff), and loaded on a HiLoad Superdex 200 (GE Healthcare) size exclusion column, pre-equilibrated with buffer A, and isocratically eluted at a 0.5 mL min<sup>-1</sup> flow rate. The fractions containing the target protein were pooled, (NH<sub>4</sub>)<sub>2</sub>SO<sub>4</sub> was added to a final concentration of 1 M, the solution was clarified by centrifugation at 48,000g for 30 min, and the supernatant was loaded on a Butyl-Sepharose High Performance (GE Healthcare) hydrophobic interaction column, pre-equilibrated with buffer A containing 1 M (NH<sub>4</sub>)<sub>2</sub>SO<sub>4</sub>. Adsorbed protein was eluted using 1–0 M (NH<sub>4</sub>)<sub>2</sub>SO<sub>4</sub> linear gradient, yielding homogeneous recombinant protein which was dialyzed against buffer A and stored at –80 °C. Pooled fractions of all purification steps were analyzed by SDS–PAGE and enzyme activity measurements. Protein concentration was determined by the method of Bradford [20] using the Bio-Rad Protein Assay Kit (Bio-Rad) and bovine serum albumin as standard.

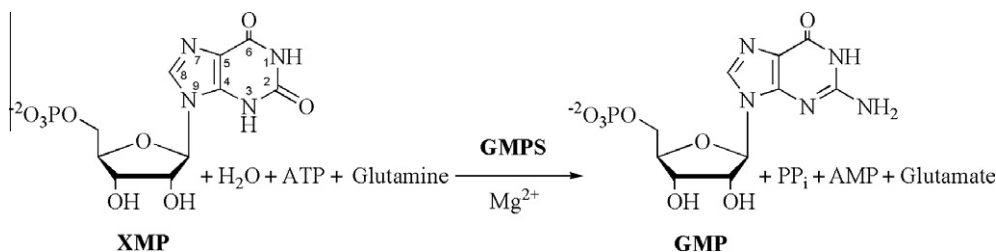


**Fig. 1.** MtGMPS catalyzes the irreversible conversion of XMP into GMP through a reaction that requires ATP and involves the transfer of an amino group from glutamine to XMP via an adenyl-XMP intermediate, generating PP<sub>i</sub>, AMP, and glutamate.

### Determination of molecular mass and oligomeric state of MtGMPS in solution

Protein identity and subunit molecular mass of homogeneous recombinant MtGMPS were assessed by mass spectrometry, and data processing carried out using the MagTran software [21]. The molecular mass of native recombinant MtGMPS was determined using a Superdex 200 HR 10/30 (GE Healthcare) size exclusion column, pre-equilibrated with 50 mM Tris pH 7.5 containing 200 mM NaCl, and a flow rate of 0.4 mL min<sup>-1</sup> was employed for isocratic protein elution. The LMW and HMW Gel Filtration Calibration Kits (GE Healthcare) were used to prepare a calibration curve. The elution volumes ( $V_e$ ) of standard proteins (ferritin, catalase, aldolase, coalbumin, ovalbumin, and ribonuclease A) were used to calculate their corresponding partition coefficient ( $K_{av}$ ; Eq. (1)). Blue dextran 2000 (GE Healthcare) was used to determine the void volume ( $V_o$ ).  $V_t$  is the total bed volume of the column. The  $K_{av}$  value for each protein was plotted against their corresponding molecular mass. Protein elution was monitored at 215, 254, and 280 nm.

$$K_{av} = \frac{V_e - V_o}{V_t - V_o} \quad (1)$$

### Apparent steady-state kinetic parameters

MtGMPS activity was continuously monitored by measuring the decrease in absorbance at 290 nm upon conversion of XMP ( $\epsilon = 3834 \text{ M}^{-1} \text{ cm}^{-1}$ ) to GMP ( $\epsilon = 2686 \text{ M}^{-1} \text{ cm}^{-1}$ ) using an UV-2550 spectrophotometer (Shimadzu). A  $\Delta\epsilon_{290}$  value of  $1148 \text{ M}^{-1} \text{ cm}^{-1}$  was employed to calculate the rate of MtGMPS-catalyzed product formation. All activity assays were performed at 40 °C in 50 mM Tris pH 7.5, unless stated otherwise, and assay mixtures contained XMP, ATP, glutamine (or  $(\text{NH}_4)_2\text{SO}_4$ ),  $\text{MgCl}_2$  (20 mM), and EDTA (0.3 mM), in a total reaction volume of 0.5 mL. Measurements of enzyme activity were initiated by the addition of 16  $\mu\text{g}$  of MtGMPS (protein concentration that yielded linear time courses). Each individual initial rate datum was the average of duplicate or triplicate measurements, and all data were analyzed by nonlinear regression using the SigmaPlot software (Systat Software, Inc.). One unit of enzyme activity (U) was defined as the amount of enzyme catalyzing the conversion of 1  $\mu\text{mol}$  of substrate into product per minute.

The pH optimum value for MtGMPS reaction was determined by measuring specific activity in 50 mM Tris buffer at pH values ranging from 6.0 to 9.5, with increments of 0.5 pH units, at 40 °C. To probe the effect of temperature on enzyme specific activity, the MtGMPS-catalyzed reaction was monitored at 25, 30, 37, and 40 °C. Both (pH and temperature) experiments were performed keeping all substrates at saturating concentrations (0.15 mM XMP, 1 mM ATP, and 5 mM glutamine) and initiated by the addition of MtGMPS into the reaction mixture.

Apparent kinetic constants for XMP, ATP, and glutamine (and  $\text{NH}_4^+$ , as  $(\text{NH}_4)_2\text{SO}_4$ ) were determined by varying the concentration of one substrate while keeping the other two at saturating concentrations. The data were either fitted to the Michaelis–Menten equation (Eq. (2)) for a hyperbolic saturation curve, to the Hill equation (Eq. (3)) for a sigmoidal saturation curve, or to the substrate inhibition equation (Eq. (4)) [22,23]. For these equations,  $v$  is the measured reaction velocity,  $V$  is the maximal velocity,  $S$  is the substrate concentration,  $K_M$  is the Michaelis constant,  $K_i$  is the dissociation constant for substrate inhibition,  $n$  is the Hill coefficient (indicating the cooperative index), and  $K_{0.5}$  is the substrate concentration in which  $v = 0.5V$ .

$$V = \frac{V[S]}{K_M + S} \quad (2)$$

$$V = \frac{V[S]^n}{K_{0.5}^n + [S]^n} \quad (3)$$

$$V = \frac{VS}{K_M + S\left(1 + \frac{S}{K_i}\right)} \quad (4)$$

### MtGMPS activity dependence on increasing $\text{Mg}^{2+}$ concentration

To investigate the influence of  $\text{Mg}^{2+}$  on MtGMPS specific activity, the enzyme-catalyzed chemical reaction was monitored at varying concentrations of  $\text{MgCl}_2$ , keeping all substrates at saturating concentrations in the presence of 0.3 mM EDTA. Apparent steady-state kinetic constants were obtained by fitting the data to the Hill equation (Eq. (3)) for a sigmoidal saturation curve. To assess whether or not there may be an additional  $\text{Mg}^{2+}$ -binding site in MtGMPS,  $\text{MgCl}_2$  was fixed at 2 mM, whereas ATP concentration was varied. Standard assay conditions were used for activity measurements, except that EDTA was omitted from the reaction mixture. Eqs. (5) and (6) were solved simultaneously to estimate  $\text{MgATP}$  concentration [24]. For these equations,  $[\text{M}]_t$ ,  $[\text{ATP}]_t$ ,  $[\text{MATP}]$ ,  $[\text{M}]$ , and  $[\text{H}]$  represent the total  $\text{Mg}^{2+}$ , total ATP, total  $\text{MgATP}^{2-}$ , free  $\text{Mg}^{2+}$ , and free hydrogen ion concentrations, respectively.  $K_1$ ,  $K_2$ , and  $K_H$  represent the dissociation constants for  $\text{MgATP}^{2-}$ ,  $\text{MgHATP}^-$ , and  $\text{HATP}^{3-}$ , respectively. The values for  $K_1$ ,  $K_2$ , and  $K_H$  were, respectively,  $1.37 \times 10^{-5}$ ,  $2 \times 10^{-3}$ , and  $1.12 \times 10^{-7}$  as given by Nakamura and Lou [14]. The MtGMPS specific activity values were plotted against  $\text{MgATP}^{2-}$ , free  $\text{Mg}^{2+}$ , and free ATP concentrations

$$[\text{M}] = [\text{M}]_t - \left([\text{MATP}] \left(1 + \frac{K_1[\text{H}]}{K_2 K_H}\right)\right) \quad (5)$$

$$[\text{MATP}] = \frac{[\text{ATP}]_t}{1 + \frac{K_1}{[\text{M}]} + \frac{K_1[\text{H}]}{[\text{M}]K_H} + \frac{K_1[\text{H}]}{K_2 K_H}} \quad (6)$$

### ATPPase activity measurements

MtGMPS ATPase activity was evaluated by the EnzCheck Pyrophosphate Assay Kit (Invitrogen), which couples the conversion of  $\text{PP}_i$  into two equivalents of inorganic phosphate ( $\text{P}_i$ ), catalyzed by inorganic pyrophosphatase, followed by phosphorolysis of 2-amino-6-mercapto-7-methylpurine ribonucleoside (MESG) catalyzed by purine nucleoside phosphorylase (PNP) to form ribose 1-phosphate and 2-amino-6-mercapto-7-methylpurine, which is detected by measuring the increase in absorbance at 360 nm ( $\epsilon = 11,000 \text{ M}^{-1} \text{ cm}^{-1}$ ) [25,26]. The reaction mixture was previously incubated for 10 min to remove any  $\text{P}_i$  contamination, and contained 50 mM Tris pH 7.5, 0.15 mM XMP, varying ATP concentration, 20 mM  $\text{MgCl}_2$ , 0.3 mM EDTA, and EnzCheck Pyrophosphate Assay Kit buffer and enzymes (PNP and inorganic pyrophosphatase) at concentrations recommended by the supplier. All reactions were initiated by the addition MtGMPS. ATP concentrations were varied in the pre-incubated reaction mixture until saturation was reached. The data were best fitted to the substrate inhibition equation (Eq. (4)).

### Isothermal titration calorimetry (ITC): measurements of ligand binding and MtGMPS glutaminase activity

ITC experiments were carried out using an iTC200 Microcalorimeter (Microcal, Inc., Northampton, MA). The reference cell (200  $\mu\text{L}$ ) was loaded with Milli Q water for all experiments and the sample cell (200  $\mu\text{L}$ ) was filled with MtGMPS at a concentration of 80  $\mu\text{M}$ . For each binding assay, the injection syringe (39.7  $\mu\text{L}$ )

contained only one ligand (1.5 mM for XMP, ATP, GMP, AMP, glutamate or PP<sub>i</sub>, or 3.5 mM for glutamine). The ligand binding isotherms were measured by direct titration (ligand into macromolecule). Recombinant MtGMPS protein was prepared for ITC experiments by dialyzing against 50 mM *N*-2-hydroxyethylpiperazine-*N'*-2-ethanesulfonic acid (Hepes) pH 7.5 containing 20 mM MgCl<sub>2</sub>. The same buffer was used to prepare all ligand solutions used in the kinetic assays, replacing Tris, which has high enthalpy of ionization [27]. The stirring speed was set to 500 rpm at a temperature of 40 °C for all experiments. The first titration injection (0.5 μL), which was discarded for data analysis, was followed by 11 injections of 3.9 μL each at 180 s intervals. Control titrations (ligand into buffer) were performed to subtract the heat of dilution and mixing for each experiment prior to data analysis. The data after peak integration of the isotherm generated by ITC were subtracted by the control titration data and concentration normalization (heat normalized to the molar ratio).

The Δ*G* (Gibbs free energy) of binding was calculated using the relationship described in Eq. (7), in which *R* is the gas constant (8.314 J K<sup>-1</sup> mol<sup>-1</sup>), *T* is the temperature in Kelvin (*T* = °C + 273.15), and *K*<sub>a</sub> is the association constant at equilibrium. The entropy of binding (Δ*S*) can also be determined by this mathematical formula. Estimates for *K*<sub>a</sub> and the binding enthalpy (Δ*H*) were refined by a standard Marquardt nonlinear regression method provided in the Origin 7 SR4 software (Microcal, Inc., Northampton, MA)

$$\Delta G^\circ = RT \ln K_a = \Delta H^\circ - T \Delta S^\circ \quad (7)$$

The observed calorimetric enthalpies (Δ*H*<sup>cal</sup>) and the rate constant for the reaction catalyzed by the MtGMPS glutaminase domain in the absence of XMP and ATP was determined from the thermograms (heat flow as a function time) obtained in the iTC200 Microcalorimeter at 40 °C. The principles of ITC implementation were described elsewhere [28]. The reaction started by the injection of 2 μL of 80 μM MtGMPS into the sample cell after 60 s of initial delay and 900 s of spacing time between the first and second injections, in a final concentration of 1.6 μM. The reaction contained 50 mM Hepes pH 7.5, 20 mM MgCl<sub>2</sub>, 5 mM glutamine, and enzyme at 80 μM initial concentration.

#### Multiple sequence alignment

The amino acid sequences of prokaryotic GMPS proteins that have three-dimensional structures solved were included in the alignment (*E. coli* (YP\_001731437.1) and *P. horikoshii* (2DPL\_B)). The human (NP\_003866.1) GMPS was also included in the alignment and compared with *M. tuberculosis* (CAB01027.1). Multiple amino acid sequence alignment was performed by Clustal W [29], using the Gonnet matrix for amino acid substitutions and considering gap penalties, to identify essential residues for nucleotide substrate(s) binding, as well as to infer possible similarities in their mechanisms of catalysis. For alignment improvement, the ATPase sequence of GMPS from *P. horikoshii* that is encoded by the *ph1347* gene, whose structure has been reported, was also analyzed.

## Results and discussion

#### *M. tuberculosis* *guaA* amplification and cloning

The *M. tuberculosis* *guaA* (Rv3396c) gene was amplified using standard PCR conditions in the presence of 5% DMSO in the reaction mixture (data not shown). The DMSO co-solvent helps overcome polymerase extension difficulties due to DNA secondary structures and improves the denaturation of GC-rich DNAs [30],

which is consistent with the 65.6% G+C content of the *M. tuberculosis* genome [9]. The PCR product consistent with the expected size (1578 bp) was purified and inserted into the pET23a(+) expression vector between the *Nde*I and *Bam*HI restriction sites. Nucleotide sequence analysis of the cloned DNA fragment confirmed the identity of the insert as the *M. tuberculosis* *guaA* coding sequence and demonstrated that no mutations were introduced by the PCR amplification step.

#### Heterologous protein expression, purification, and mass spectrometry of homogeneous MtGMPS

MtGMPS was overexpressed in *E. coli* BL21(DE3) electrocompetent host cells transformed with the pET-23a(+):*guaA* recombinant plasmid. SDS-PAGE analysis confirmed the expression of a protein in the soluble fraction with apparent subunit molecular mass consistent with the one expected for MtGMPS (approximately 56 kDa), and showed that the highest yield of soluble recombinant MtGMPS expression was obtained at 6 h of cell growth after reaching an OD<sub>600nm</sub> = 0.4–0.6 at 37 °C in LB medium (Fig. S1, Supplementary Data), without IPTG addition. In the pET vector system, target genes are positioned downstream of the strong bacteriophage T7 late promoter. In agreement with the results presented here, high levels of protein expression in the absence of inducer have been shown to occur in the pET system [31–33]. It has been proposed that leaky protein expression is a property of the *lac*-controlled system when cells approach stationary phase in complex medium and that cyclic adenosine monophosphate, acetate, and low pH are required to achieve high-level expression in the absence of IPTG induction, which may be part of the general cellular response to nutrition limitation [34]. However, more recently, it has been shown that unintended induction in the pET system is due to the presence of as little as 0.0001% of lactose in the medium [35].

The overexpressed recombinant MtGMPS protein was purified by a three-step protocol consisting of an anion exchange column (Q-Sepharose Fast Flow), a size exclusion column (HiLoad Superdex 200), and a hydrophobic interaction column (Butyl-Sepharose High Performance). SDS-PAGE analysis showed that MtGMPS was apparently homogeneous (Fig. S2, Supplementary Data). This purification protocol yielded 10 mg of homogeneous recombinant protein from 2 g of wet cell paste, with an overall protein yield of 32% (Table S1, Supplementary Data). Mass spectrometry analysis was carried out to show identity and integrity of homogeneous recombinant MtGMPS. Mass spectrometry analysis of trypsin-digested MtGMPS identified 82% of the enzyme primary sequence (Table S2, Supplementary Data). Deconvoluted spectra of MtGMPS presented a single peak corresponding to an average subunit molecular mass value of (55,928.64 Da), suggesting removal of the N-terminal methionine residue (theoretical = 56,027.60 Da) (Fig. S3, Supplementary Data). The mass spectrometry analysis also revealed no peak at the expected mass of *E. coli* GMPS (58,679 Da), thus lending further support for homogeneity of recombinant protein. Recombinant MtGMPS was stored at –80 °C in 50 mM Tris pH 7.5, as this buffer was found to be appropriate for further steady-state enzyme activity measurements. No loss on specific activity could be observed after storage for at least three months at this temperature (data not shown).

#### Oligomeric state of MtGMPS

The molecular mass of native MtGMPS was determined by size exclusion chromatography and yielded a single peak with elution volume (12.35 mL) corresponding to 136.96 kDa, suggesting that MtGMPS is a dimer in solution (136,960 Da/55928.64 Da ≈ 2.4). This result is in agreement with the oligomeric state of GMPS

proteins from *E. coli* [16], *P. falciparum* [15], and *P. horikoshii* [17], but differs from higher eukaryotes, including humans [14], which are monomeric. The presence of a large insertion near the dimerization domain in GMPS of higher eukaryotes seems to preclude dimer formation [36]. It has been suggested that the diversity in oligomeric states of this class of enzyme may reflect different modes of regulation and varied functions [15].

#### Apparent steady-state kinetics

Prior to embarking on determining the apparent steady-state kinetic parameters, the optimum pH value was determined. MtGMPS activity measurements at saturating substrate concentrations showed that the optimum pH value was 7.5 (Fig. 2). To allow comparisons to be made between velocities of MtGMPS, human [14], and *E. coli* [16,37] enzymes, specific activity values were determined at various temperatures. Not surprisingly, MtGMPS specific activity increased as a function of temperature up to 40 °C (data not shown). Steady-state velocity measurements were thus carried out at 40 °C in 50 mM Tris pH 7.5.

Saturations curves for MtGMPS specific activity plotted against increasing concentrations of XMP (Fig. 3A), ATP (Fig. 3B), glutamine (Fig. 3C), and  $\text{NH}_4^+$  (Fig. 3C-inset) showed to obey distinct functions. The apparent steady-state kinetic parameters are given in Table 1. Fitting the sigmoidal data for XMP saturation curve to Eq. (3) yielded values of  $45 (\pm 1) \mu\text{M}$  for the Hill constant ( $K_{0.5}$ ) and  $2.30 (\pm 0.04) \text{ s}^{-1}$  for  $k_{\text{cat}}$ , suggesting positive homotropic cooperative kinetics for XMP. A similar pattern has also been observed for human GMPS isozymes, which have  $K_{0.5}$  values of 35.6 and  $45.4 \mu\text{M}$  [14]. Interestingly, to the best of our knowledge, a sigmoidal profile for XMP saturation curve has never been observed for GMPS enzymes of prokaryotes. Increasing XMP concentrations resulted in inhibition of MtGMPS activity (data not shown). The limiting value for the Hill coefficient ( $n$ ) is 2 as MtGMPS is a dimer in solution. The  $n$  value of 2.4 thus indicates strong positive homotropic cooperativity for XMP.

The saturation curve for  $\text{NH}_4^+$  was also sigmoidal (Fig. 3C-inset) and fitting the data to Eq. (3) yielded values of  $13 (\pm 1) \text{ mM}$  for  $K_{0.5}$  and  $1.02 (\pm 0.04) \text{ s}^{-1}$  for  $k_{\text{cat}}$  (Table 1). Interestingly, saturation curves for increasing  $\text{NH}_4^+$  concentrations were shown to be hyperbolic for human ( $K_M = 5.1 \text{ mM}$ ) [14], *E. coli* ( $K_M = 41$  or  $293 \text{ mM}$ ) [37], and *P. falciparum* ( $K_M = 5.4 \text{ mM}$ ) [15] GMPS enzymes. As shown for human GMPS [14], the catalytic constant is significantly

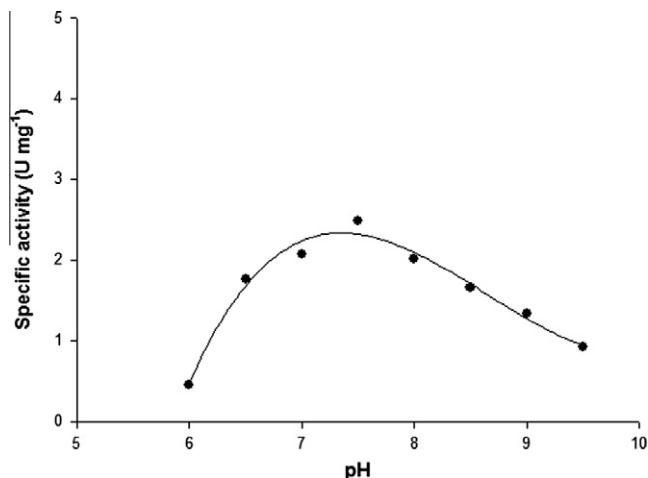


Fig. 2. Screening of MtGMPS specific activity as a function of pH. The experiment was carried out in 50 mM Tris buffer at pH values ranging from 6.0 to 9.5, with increments of 0.5 pH units, at 40 °C.

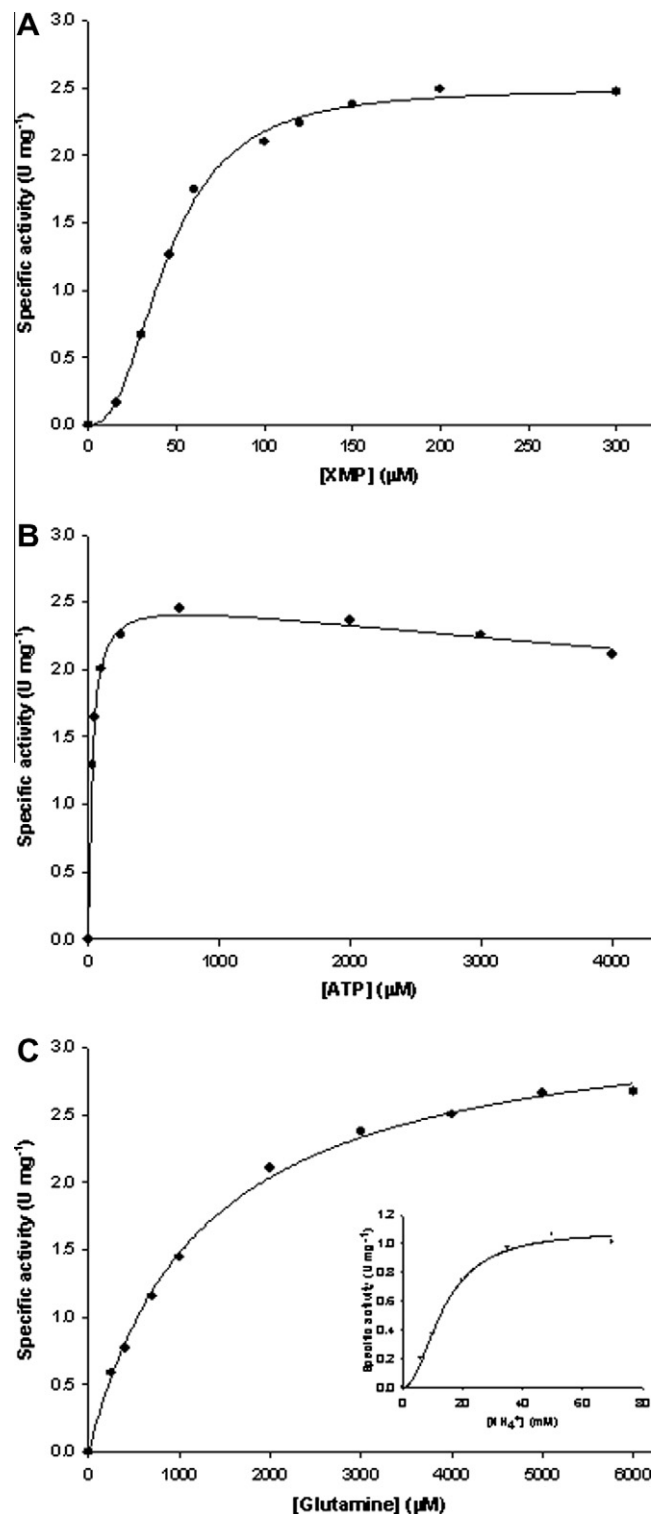


Fig. 3. Apparent kinetic parameters for MtGMPS. Specific activity as a function of the concentration of (A) XMP, (B) ATP, and (C) glutamine. Inset displays the specific activity as a function of ammonia.

lower for  $\text{NH}_4^+$  ( $k_{\text{cat}} = 0.10 \text{ s}^{-1}$ ) as compared to glutamine ( $k_{\text{cat}} = 3.05 \text{ s}^{-1}$ ; Table 1), suggesting that the latter is likely to be the preferred physiological substrate for MtGMPS. The  $K_M$  value for glutamine (1.24 mM), derived from fitting the hyperbolic saturation curve data (Fig. 3C) to Eq. (2), is smaller than that found for *E. coli* GMPS (13 mM) [37] and larger than those for human GMPS isozymes (406 and 358  $\mu\text{M}$ ) [14].

**Table 1**

Apparent kinetic constants for MtGMPS at varying XMP, ATP, glutamine, and  $\text{NH}_4^+$  concentrations.

	$K_{0.5}$ ( $\mu\text{M}$ )	$K_M$ ( $\mu\text{M}$ )	$V_{\max}$ ( $\text{U mg}^{-1}$ )	$k_{\text{cat}}$ ( $\text{s}^{-1}$ )
XMP	$45 \pm 1$	–	$2.49 \pm 0.04$	$2.30 \pm 0.04$
ATP	–	$27 \pm 2$	$2.58 \pm 0.04$	$2.39 \pm 0.04$
Glutamine	–	$1.24 (\pm 0.06) \times 10^3$	$3.30 \pm 0.05$	$3.05 \pm 0.05$
$\text{NH}_4^+$	$13 \pm 1^*$	–	$1.10 \pm 0.04$	$1.02 \pm 0.04$

\* The  $K_M$  for  $\text{NH}_4^+$  is given in mM.

The saturation curve for ATP in the presence of saturating concentrations of XMP and glutamine showed reduced MtGMPS activity at large (post-saturating) concentrations of ATP (Fig. 3B). Accordingly, these data were fitted to Eq. (4), yielding  $K_M$  and  $k_{\text{cat}}$  values of  $27 (\pm 2) \mu\text{M}$  and  $2.39 (\pm 0.04) \text{s}^{-1}$ , respectively, for ATP (Table 1). The substrate inhibition constant ( $K_i$ ) was  $21 \pm 3 \text{mM}$  for ATP, which is approximately 780-fold larger than the  $K_M$  (Table 1). A similar profile was observed for the mycobacterial enzyme that catalyzes the previous step in the pathway, IMPDH [10]. Substrate inhibition of *M. tuberculosis* IMPDH was attributed to the formation of an IMPDH-XMP $\cdot$ :NAD complex, which is an intermediate of the reaction [38,39].

#### Activity dependence on $\text{Mg}^{2+}$ concentration

To evaluate the  $\text{Mg}^{2+}$  metal requirement of MtGMPS, enzyme activity measurements were carried out at increasing metal concentrations. The  $\text{Mg}^{2+}$  saturation curve was apparently sigmoidal and the data were best fitted to Eq. (3) (Fig. 4A), yielding a value of a value of 2.67 for the Hill coefficient ( $n$ ),  $1.18 \pm 0.03 \text{mM}$  for  $K_{0.5}$ , and  $1.96 \pm 0.02 \text{s}^{-1}$  for  $k_{\text{cat}}$ . These data suggest strong positive homotropic cooperativity upon increasing concentrations of  $\text{Mg}^{2+}$ . Maximum specific activity was achieved at approximately 5 mM  $\text{Mg}^{2+}$ , which is 5-fold larger than the concentration of ATP (1 mM) in the reaction mixture, suggesting that there may be an additional binding site for  $\text{Mg}^{2+}$  in MtGMPS. Sigmoidal dependence of enzyme activity on increasing  $\text{Mg}^{2+}$  concentration has also been observed for human GMPS [14] and *E. coli* GMPS [37]. To try to ascertain whether or not there is an additional  $\text{Mg}^{2+}$  binding site in MtGMPS, ATP was varied in the presence of  $\text{Mg}^{2+}$  at a fixed concentration of 2 mM (Fig. 4B), in the absence of EDTA. It is noteworthy that the maximum enzyme activity was not achieved at the maximum MgATP concentration. In addition, after a maximum value of  $\sim 2.5 \text{U mg}^{-1}$ , the MtGMPS specific activity decreased as free  $\text{Mg}^{2+}$  concentration decreased (Fig. 4B). These data suggest that either free ATP competes for the MgATP binding site, which is also consistent with the product inhibition showed in Fig. 3B, or that the enzyme has an additional site for free  $\text{Mg}^{2+}$ , whose occupancy results in increasing enzyme activity. Although additional binding sites for free  $\text{Mg}^{2+}$  have been proposed for human [14] and *E. coli* [37] GMPS proteins, whether or not there exists an additional binding for free  $\text{Mg}^{2+}$  should await experimental evidence on MtGMPS structure. At any rate, enzyme activity measurements to determine the apparent steady-state kinetic parameters for XMP, ATP, glutamine, and  $\text{NH}_4^+$  were carried out at fixed-saturating concentration of  $\text{MgCl}_2$  (20 mM).

#### ATPPase activity of MtGMPS

GMPS proteins consist of two catalytic units, a GATase domain and an ATPase domain. The GATase domain has glutaminase activity. The ATPase domain binds ATP and XMP, in the presence of  $\text{Mg}^{2+}$ , to form the activated adenyl-XMP intermediate with concomitant  $\text{PP}_i$  formation [15,36,37]. As an attempt to determine whether or not the ATPase activity of MtGMPS is independent

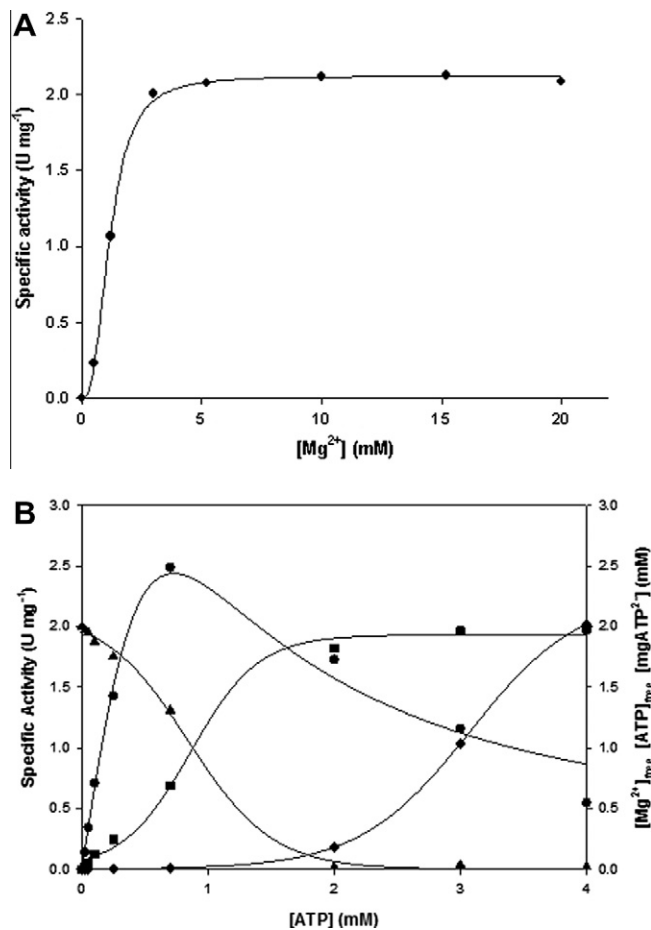


**Fig. 4.** MtGMPS enzyme activity dependence on  $\text{Mg}^{2+}$ . All the assays were performed using standard conditions, as described in the Section 2. (A) Activity of MtGMPS with respect to  $\text{Mg}^{2+}$ , at a fixed concentration of ATP (2 mM). These data were best fitted the positive cooperativity equation (Eq. (3)). (B) Effect of varying ATP concentration on MtGMPS activity at fixed concentration of  $\text{Mg}^{2+}$  (2 mM), in which (●) represents MtGMPS specific activity in  $\text{U mg}^{-1}$ , (■)  $[\text{MgATP}^{2-}]$ , (◆) free  $[\text{ATP}]$ , and (▲) free  $[\text{Mg}^{2+}]$ .

of GATase activity, measurements of  $\text{PP}_i$  formation were carried out by a coupled assay with PNP and pyrophosphatase in the absence of glutamine and fixed-saturating concentration of XMP (0.15 mM). The data (Fig. 5) were best fitted to the substrate inhibition equation (Eq. (4)), yielding values of  $56 (\pm 6) \mu\text{M}$  for  $K_M$ ,  $0.71 (\pm 0.02) \text{s}^{-1}$  for  $k_{\text{cat}}$ , and  $9 (\pm 2) \text{mM}$  for  $K_i$ . These results suggest formation of adenyl-XMP with concomitant release of  $\text{PP}_i$  in the absence of glutamine. The  $K_M$  values in either the absence ( $56 \mu\text{M}$ ) or presence ( $27 \mu\text{M}$ ) of glutamine are somewhat similar, whereas the  $k_{\text{cat}}$  value in the presence of glutamine ( $2.39 \text{s}^{-1}$ ) is larger than in the absence of glutamine ( $0.71 \text{s}^{-1}$ ). These data suggest that glutamine has no effect on the overall dissociation constant of ATP, whereas it appears to increase the overall catalytic rate of the ATPase domain of MtGMPS.

#### ITC: ligand binding and glutaminase activity

In order to determine the true steady-state kinetic parameters and initial velocity patterns in double-reciprocal plots for MtGMPS, enzyme activity measurements were made in the presence of varying glutamine (100–5055  $\mu\text{M}$ ) concentrations and several fixed-varied ATP (100–2000  $\mu\text{M}$ ) concentrations, while keeping XMP at a fixed (150  $\mu\text{M}$ ) concentration. However, the double-reciprocal plots were curved upwards for ATP and showed a non-consistent

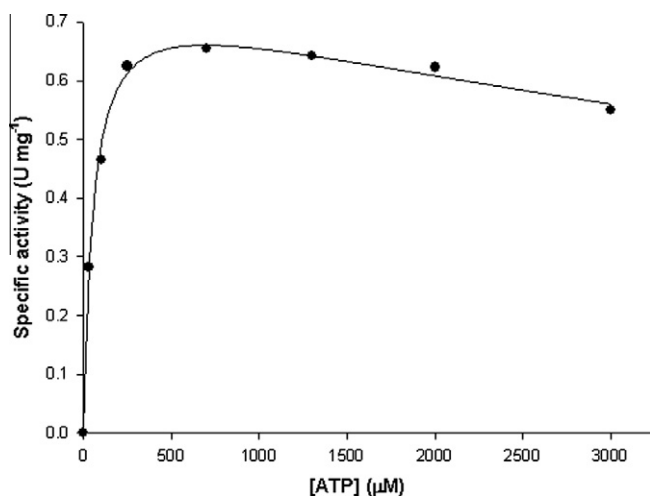


Fig. 5. MtGMPS specific activity as a function of ATP concentration without glutamine in the reaction mixture reveals the release of  $PP_i$  and the formation of adenylyl-XMP.

dependence on increasing glutamine concentration (data not shown), thereby precluding a proposal for MtGMPS enzyme mechanism based on measurements of dependence of steady-state velocities on increasing ATP or glutamine concentrations. In addition, the dependence of MtGMPS on increasing XMP concentration was sigmoidal.

To try to address the order of substrate addition and/or product release, equilibrium binary complex formation were assessed by ITC, determining the heat generated or consumed upon ligand-macromolecule binary complex formation at constant temperature and pressure (Fig. 6). The ITC data also provide thermodynamic signatures of non-covalent interactions of substrate(s)/product(s) binding to MtGMPS. The measure of heat released upon binding of the ligands allowed the determination of the binding enthalpy ( $\Delta H$ ) of the process, the stoichiometry of the interaction ( $n$ ), and the association constant at equilibrium ( $K_a$ ). The dissociation constant at equilibrium ( $K_d$ ) could be calculated as the inverse of  $K_a$  ( $K_d = 1/K_a$ ). Furthermore, the Gibbs free energy ( $\Delta G$ ) and entropy of binding ( $\Delta S$ ) were determined from the association constant values at equilibrium as described by Eq. (7). The overall binding isotherms for XMP, ATP, and glutamine were best fitted to a model of one set of sites assuming that the substrates bind to the monomer with the same affinity in all active sites (Table 2). The rather large standard errors were a direct consequence of the shape of the binding isotherm, which will dictate how accurate the thermodynamic parameters can be determined. The shape of the binding isotherm is dependent on  $K_d$  and the concentration of the interacting component in the calorimeter cell (the total binding site concentration) [28,33]. The product of these two terms gives a number called the C value, which is given by  $C = nK_B[\text{component 2}]$ , where  $n$  represents the stoichiometry of the interaction,  $K_B$  is the equilibrium binding constant and [component 2] the total concentration of binding sites. The latter is limited by the need to obtain large quantities and/or solubility. In the concentrations regimes usually adopted for ITC experiments, the data sets with low C values tend to rather featureless lines due to little changes in  $\Delta H$  values from injection to injection. As it is important to obtain an isotherm that provides maximum data points for the fitting process, the loss of the plateau at the beginning of the titration curve due to low C values might have contributed to the large standard errors.

The  $PP_i$  binding isotherm (Fig. 6D) was not sufficiently defined to provide an adequate fit of the data to any model, probably

because this substrate may exert different and simultaneous effects on MtGMPS. Moreover, the rather large temperature (40 °C) in the assay generated an elevated dilution heat, affecting the reading and collection of constants. At any rate, binding of  $PP_i$  to free MtGMPS could be detected by ITC measurements (Fig. 6D). The ITC results show that XMP (Fig. 6A) and ATP (Fig. 6B) bind to the free enzyme in the presence of  $Mg^{2+}$ , which suggests a random mechanism of binding of both substrates to the ATPase domain of MtGMPS. Glutamine, the substrate hydrolyzed by the GATase domain of MtGMPS, binds to free enzyme (Fig. 6C). No binding of either GMP, AMP, or glutamate to free enzyme could be detected by ITC (insets of Fig. 6A, B, and C, respectively). The ITC data thus suggest that substrate binding is random and  $PP_i$  is the last product to be released to yield free enzyme. However, an order for release of glutamate, AMP, and GMP could not be derived from the ITC data. An ordered mechanism has been proposed for human GMPS [37], in which MgATP binding is followed by XMP, and glutamine is the last substrate to bind, whereas  $PP_i$  is the last product to be released to yield free enzyme. A steady-state ordered addition of MgATP followed by XMP to ATPase domain of *P. falciparum* GMPS has been proposed based on product inhibition studies [15]. In addition, glutamine binding to *P. falciparum* GMPS enzyme appears to be independent of the binding of ATP and XMP, as for MtGMPS, and glutamate is the first product to be released, followed by AMP, GMP, and  $PP_i$  [15]. On the other hand, a different order of substrate binding has been proposed based on the crystal structure of *E. coli* GMPS, in which XMP binding is followed by MgATP, and glutamine is the last substrate to bind to the enzyme [36].

The glutaminase activity assay was carried out to determine whether hydrolysis of glutamine to  $NH_3$  and glutamate occurs in the absence of XMP and ATP. Although the ITC data showed that glutamine binds to free MtGMPS, no glutaminase activity could be detected in the absence of XMP and ATP. To achieve the enzymatic conformation for hydrolysis of glutamine, it is necessary for XMP and ATP substrates to be present in the binding site [14,36]. This is consistent with the proposal that GMPS has poor glutaminase activity in the absence of XMP and ATP to guarantee that hydrolysis of glutamine is tightly coupled with product formation, thereby preventing indiscriminate conversion of glutamine to  $NH_3$  and glutamate [15,36]. Formation of adenylyl-XMP reaction intermediate in the ATPase domain has been proposed to signal the glutaminase domain for complete activity, leading to channeling of  $NH_3$  formed in the GATase to ATPase domain only in the presence of adduct in the latter [15].

#### Multiple sequence alignment

The polypeptide sequences of prokaryotic and eukaryotic GMPSs, to which three-dimensional structures have been reported, were included in the primary sequence comparison analysis carried out using Clustal W (Fig. 7). Namely, the two-domain type GMPS proteins from *E. coli* (PDB ID: 1GPM) [36] and *Homo sapiens* (PDB ID: 2VXO; Welin et al., unpublished results), and the ATPase subunit of two-subunit type GMPS protein from the hyperthermophilic archaeon *P. horikoshii* OT3 (PDB ID: 3A4I) [17]. This analysis suggests that the residues of the Cys-His-Glu catalytic triad in the N-terminal Class I amidotransferase domain of *E. coli* GMPS [36] are conserved in MtGMPS, namely Cys93, His179, and Glu181 (*M. tuberculosis* numbering) (Fig. 7). By analogy to many hydrolytic enzymes, it has been proposed that the His residue of the Cys-His-Glu catalytic triad serves as a general base in the nucleophilic attack of Cys side chain on the amide carbon of glutamine [36]. In addition, MtGMPS contains a glycine-rich ATP-binding motif called the “P-loop” (residues 233–239; SGGVDSS) (Fig. 7), which is strictly conserved in the ATPase subunits/domains of GMPS proteins [17,36].

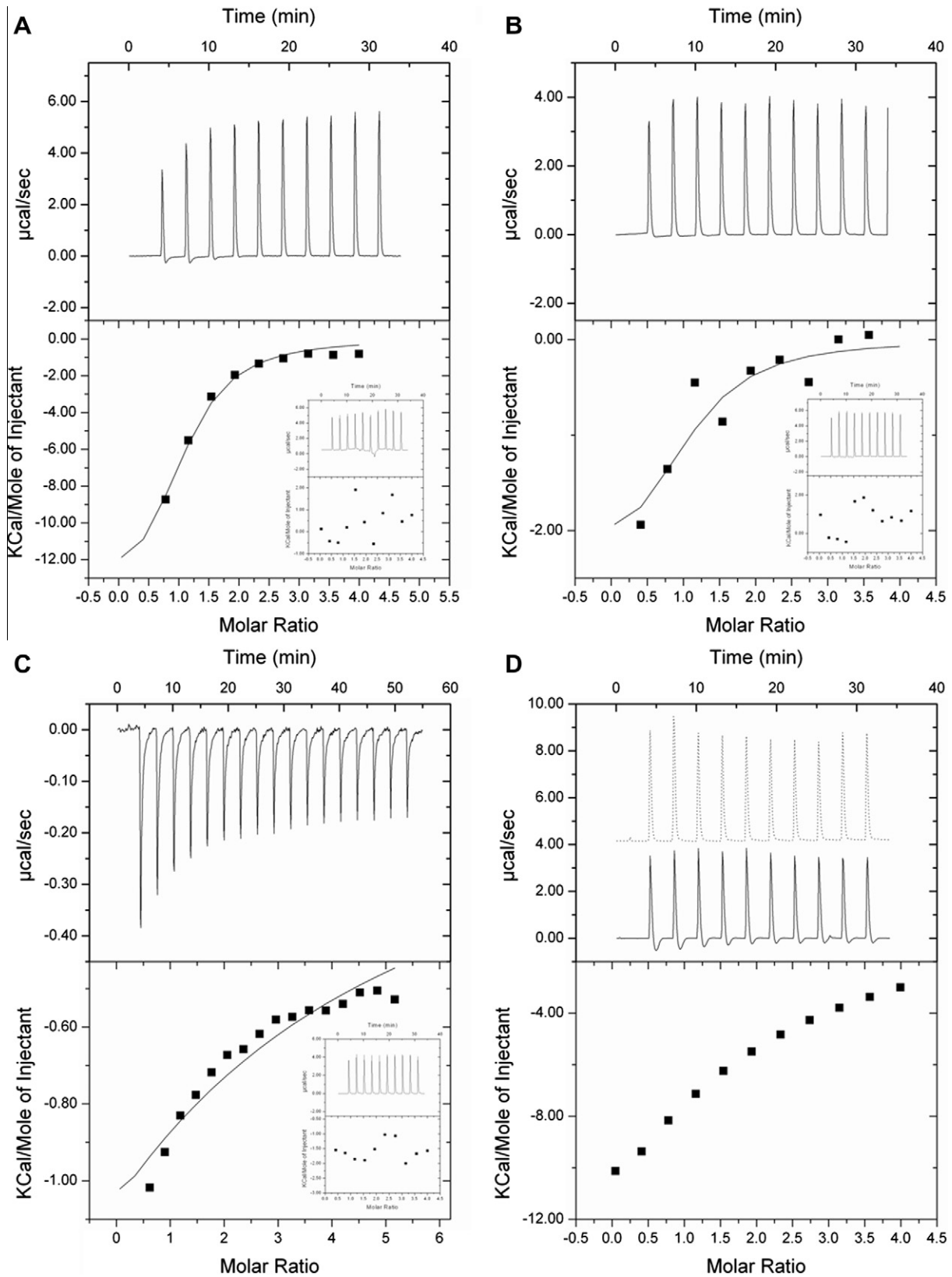


**Fig. 6.** Isothermal titration calorimetric (ITC) curves for binding of ligands to MtGMPs (80  $\mu$ M). (A) Titration of XMP at a final concentration of 1.5 mM. (B) Titration of ATP at a final concentration of 1.5 mM. (C) Titration of glutamine at a final concentration of 3.5 mM. (D) Titration of PP<sub>i</sub> at a final concentration of 1.5 mM. The insets are titration of (A) GMP, (B) AMP, and (C) glutamate, respectively. The same scale was employed for the Y-axis of large panels and insets.

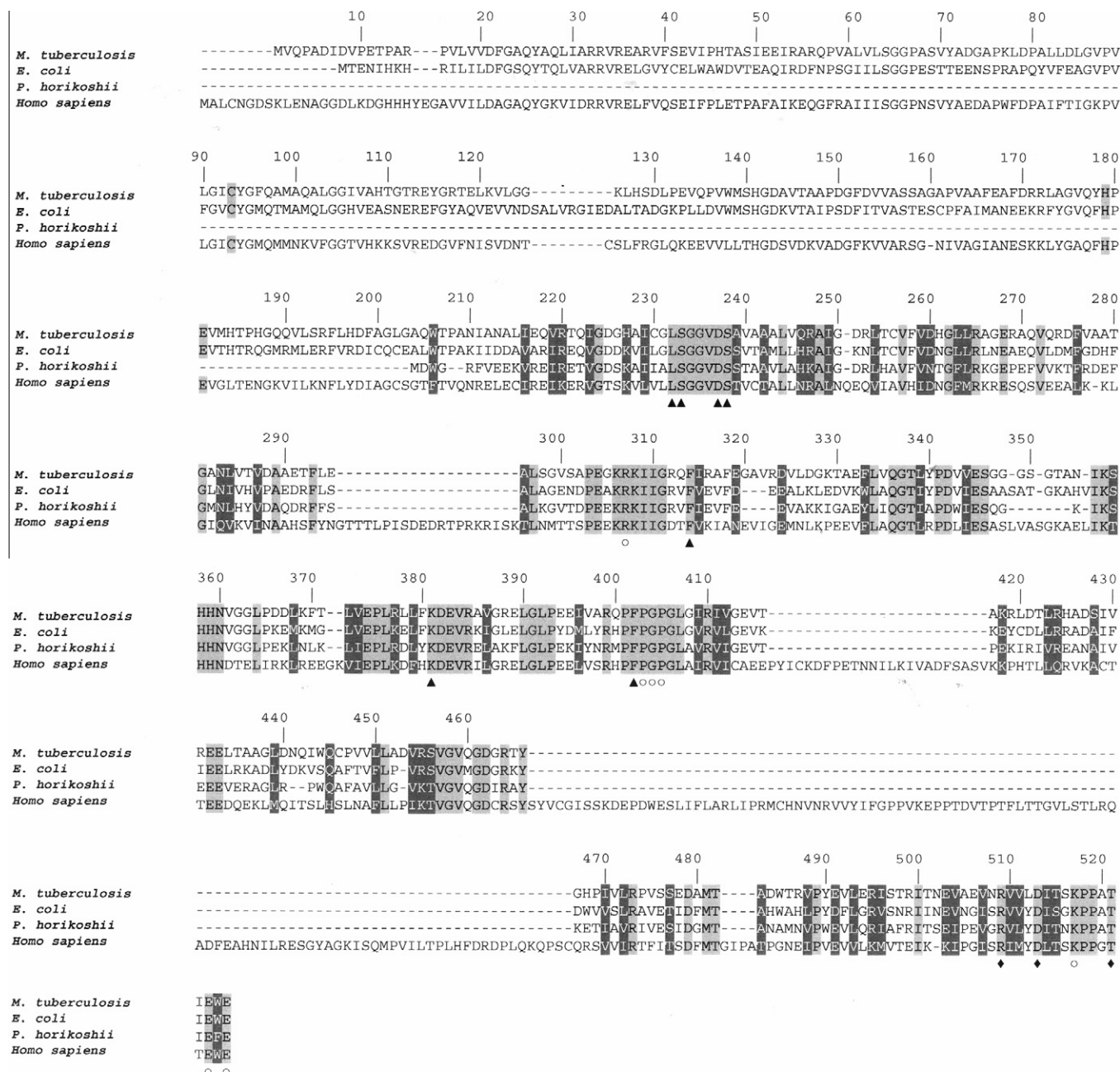
These results suggest that MtGMPs belongs to N-type ATP pyrophosphatase family. The members of this family have structurally

homologous ATP-binding domains and a common mechanism in which the carboxyl or carbonyl groups are activated by adenylation.

**Table 2**

Association constants and thermodynamic parameters of different ligands binding to MtGMPS.

Ligands	<i>n</i>	$\Delta H^\circ$ (kcal mol <sup>-1</sup> )	$\Delta G^\circ$ (kcal mol <sup>-1</sup> )	$\Delta S^\circ$ (cal mol <sup>-1</sup> K <sup>-1</sup> )	<i>K<sub>d</sub></i> (M)
XMP	1	-14.9 ± 0.6	-7 ± 4	-25.1	18 (±3) × 10 <sup>-6</sup>
ATP	1	-3 ± 5	-7 ± 5	13.0	24 (±18) × 10 <sup>-6</sup>
Glutamine	1	-16 ± 2	-3.4 ± 0.4	-39.6	2.0 (±0.3) × 10 <sup>-3</sup>

*n* = number of sites,  $\Delta H$  = binding enthalpy,  $\Delta G$  = Gibbs free energy,  $\Delta S$  = binding entropy, *K<sub>d</sub>* = equilibrium dissociation constant.**Fig. 7.** Multiple sequence alignment of polypeptide chains of GMPS enzymes. Completely and highly conserved residues are boxed and indicated by black letters on a gray background and white letters on a gray background, respectively. Triangles and circles indicate the putative binding residues for ATP and XMP, respectively. Diamonds indicate residues forming intermolecular hydrogen bonds in homodimers of *P. horikoshii* (ATPase domain), *E. coli*, and *M. tuberculosis* GMPS enzymes. Sequence alignment was obtained with Clustal W.

tion (releasing PP<sub>i</sub>) followed by attack of a nitrogen nucleophile releasing AMP [36]. The largest differences between the primary sequences of prokaryotic and eukaryotic GMPS proteins map to

the C-terminal amino acids of the dimerization domain [36]. Monomeric eukaryotic GMPS has several large insertions as compared to prokaryotes, which are thought to form an additional

domain that eliminates the need for dimerization. The residues Arg509, Val510, Tyr512, Asp513, and Thr521, which form intermolecular hydrogen bonds, are conserved in *P. horikoshii* and *E. coli* (Fig. 7). These residues are also conserved in *M. tuberculosis* and humans with the exception of Val510 (Ile in humans) and Leu512 in *M. tuberculosis*, which are obviously not involved in dimerization in the crystal (PDB ID: 2VXO) of monomeric human GMPS [14]. The dimerization domain is adjacent to the ATP-binding site of the ATPase domain. Contacts between the domains are highly conserved, including the proline- and glycine-rich linker peptide (residues 403–408), which in *E. coli* (PDB ID: 1GPM) is anchored in the dimerization domain by the specific contacts of invariant residues [36]. On the other hand, all residues of the putative XMP-recognizing amino acid residues are conserved between the polypeptide sequences included in the alignment (Fig. 7). MtGMPS has fairly high identity to prokaryotic GMPSs (*M. tuberculosis* and *E. coli* GMPSs: 47.39%; *M. tuberculosis* and *P. horikoshii* GMPSs: 31.81%), and relatively low identity to the human protein (*M. tuberculosis* and human GMPSs: 15.50%).

## Conclusions

Particular features of *M. tuberculosis*, such as enzymes of either essential metabolic pathways exclusive to the microorganism [40] or nucleotide salvage pathways [12,41] with unique characteristics as compared to the human host can be explored to direct efforts towards developing new strategies to combat TB. Purine biosynthetic enzymes, including MtGMPS, are considered to be attractive targets for the development of new auxotrophic strains or novel anti-mycobacterial agents [8,12,13,42]. Although the *guaA* gene has been predicted by *in silico* analysis of *M. tuberculosis* genome sequence to encode a protein with GMPS activity, no formal biochemical data have been presented to lend support to this computational prediction. To pave the way for further efforts to show whether or not deletion of the *guaA* gene may result in an auxotrophic *M. tuberculosis* strain with attenuated virulence, the present work presents biochemical data on *guaA*-encoded MtGMPS.

Vaccines are widely recognized to be one of the most important medical advances in history. However, the field of TB vaccine faces formidable scientific and policy challenges. A recently published study undertaken by Aeras to assess the barriers and drivers to the introduction of new TB vaccines arrived at the following conclusions [43]: “a collaborative approach to solving scientific, policy, and resource obstacles – as well as new partnerships among emerging economies and vaccine development organizations – will be critical to developing a new TB vaccine that could achieve its public health potential to save lives and reduce the burden of disease”. Accordingly, the work reported here represents a first step towards further efforts to show whether or not deletion of the *guaA* gene may result in an auxotrophic *M. tuberculosis* strain with attenuated virulence. It is also hoped that the biochemical data here presented may contribute to functional genomic efforts. In addition, understanding the mode of action of MtGMPS may be useful to chemical biologists interested in designing function-based chemical compounds to elucidate the biological role of this enzyme in the context of whole *M. tuberculosis* cells.

## Acknowledgments

This work was supported by funds of Decit/SCITIE/MS-MCT-CNPq-FNDCT-CAPES to National Institute of Science and Technology on Tuberculosis (INCT-TB) to D.S.S. and L.A.B. L.A.B. and D.S.S. also acknowledge financial support awarded by FAPERGS-CNPq-PRONEX-2009. D.S.S. (CNPq, 304051/1975-06) and L.A.B. (CNPq, 520182/99-5) and are Research Career Awardees of the National

Research Council of Brazil (CNPq). T.M.A.F., D.C.R., R.G.D., and D.M.L. acknowledge scholarships awarded by CNPq.

## Appendix A. Supplementary data

Supplementary data associated with this article can be found, in the online version, at doi:10.1016/j.abb.2011.11.013.

## References

- [1] World Health Organization, Multidrug and extensively drug-resistant TB (M/XDR-TB): 2010 global report on surveillance and response, WHO/HTM/TB/2010.3, 2010.
- [2] W.W. Yew, C.C. Leung, *Respirology* 13 (2008) 21–46.
- [3] A.A. Velayati, P. Farnia, M.R. Masjedi, T.A. Ibrahim, P. Tabarsi, R.Z. Haroun, H.O. Kuan, J. Ghanavi, P. Farnia, M. Varahram, *Eur. Respir. J.* 34 (2009) 1202–1203.
- [4] R.G. Ducati, A. Ruffino-Netto, L.A. Basso, D.S. Santos, *Mem. Inst. Oswaldo Cruz* 101 (2006) 697–714.
- [5] B.B. Trunz, P. Fine, C. Dye, *Lancet* 367 (2006) 1173–1180.
- [6] K.L. Kotloff, M.F. Pasetti, E.M. Barry, J.P. Nataro, S.S. Wasserman, M.B. Szein, W.D. Picking, M.M. Levine, *J. Infect. Dis.* 190 (2004) 1745–1754.
- [7] K.L. Kotloff, J.K. Simon, M.F. Pasetti, M.B. Szein, S.L. Wooden, S. Livio, J.P. Nataro, W.C. Blackwelder, E.M. Barry, W. Picking, M.M. Levine, *Hum. Vaccin.* 3 (2007) 268–275.
- [8] A.E. Santiago, L.E. Cole, A. Franco, S.N. Vogel, M.M. Levine, E.M. Barry, *Vaccine* 27 (2009) 2426–2436.
- [9] S.T. Cole, R. Brosch, J. Parkhill, T. Garnier, C. Churcher, D. Harris, S.V. Gordon, K. Eiglmeier, S. Gas, C.E. Barry 3rd, F. Tekaiia, K. Badcock, D. Basham, D. Brown, T. Chillingworth, R. Connor, R. Davies, K. Devlin, T. Feltwell, S. Gentles, N. Hamlin, S. Holroyd, T. Hornsby, K. Jagels, A. Krogh, J. McLean, S. Moule, L. Murphy, K. Oliver, J. Osborne, M.A. Quail, M.A. Rajandream, J. Rogers, S. Rutter, K. Seeger, J. Skelton, R. Squares, S. Squares, J.E. Sulston, K. Taylor, S. Whitehead, B.G. Barrell, *Nature* 393 (1998) 537–544.
- [10] L. Chen, D.J. Wilson, Y. Xu, C.C. Aldrich, K. Felczak, Y.Y. Sham, K.W. Pankiewicz, *J. Med. Chem.* 53 (2010) 4768–4778.
- [11] V. Kamalakannan, G. Ramachandran, S. Narayanan, S.K. Vasan, P.R. Narayanan, *FEMS Microbiol. Lett.* 209 (2002) 261–266.
- [12] R.G. Ducati, A. Breda, L.A. Basso, D.S. Santos, *Curr. Med. Chem.* 18 (2011) 1258–1275.
- [13] M. Hirst, E. Haliday, J. Nakamura, L. Lou, *J. Biol. Chem.* 269 (1994) 23830–23837.
- [14] J. Nakamura, L. Lou, *J. Biol. Chem.* 270 (1995) 7347–7353.
- [15] J.Y. Bhat, B.G. Shastri, H. Balaram, *Biochem. J.* 409 (2008) 263–273.
- [16] J.L. Abbott, J.M. Newell, C.M. Lightcap, M.E. Olanich, D.T. Loughlin, M.A. Weller, G. Lam, S. Pollack, W.A. Patton, *Protein J.* 25 (2006) 483–491.
- [17] S. Maruoka, S. Horita, W.C. Lee, K. Nagata, M. Tanokura, *J. Mol. Biol.* 395 (2010) 417–429.
- [18] C.M. Sasseti, D.H. Boyd, E.J. Rubin, *Mol. Microbiol.* 48 (2003) 77–84.
- [19] U.K. Laemmli, *Nature* 227 (1970) 680–685.
- [20] M.M. Bradford, *Anal. Biochem.* 72 (1976) 248–254.
- [21] Z. Zhang, A.G. Marshall, *J. Am. Soc. Mass Spectrom.* 9 (1998) 225–233.
- [22] I. Segel, *Enzyme, Kinetics Behavior and Analysis of Rapid Equilibrium and Steady-state Enzyme Systems*, John Wiley and Sons, New York, 1975.
- [23] R.A. Copeland, *Evaluation of Enzyme Inhibitors in Drug Discovery*, John Wiley and Sons, Inc., New Jersey, 2005.
- [24] J.G. Robertson, J.J. Villafranca, *Biochemistry* 32 (1993) 3769–3777.
- [25] M.R. Webb, *Proc. Natl. Acad. Sci. USA* 89 (1992) 4884–4887.
- [26] R.G. Ducati, D.S. Santos, L.A. Basso, *Arch. Biochem. Biophys.* 486 (2009) 155–164.
- [27] D.C. Rostirolla, A. Breda, L.A. Rosado, M.S. Palma, L.A. Basso, D.S. Santos, *Arch. Biochem. Biophys.* 505 (2011) 202–212.
- [28] M.L. Bianconi, *J. Biol. Chem.* 278 (2003) 18709–18713.
- [29] J.D. Thompson, D.G. Higgins, T.J. Gibson, *Nucleic Acids Res.* 22 (1994) 4673–4680.
- [30] P.R. Winship, *Nucleic Acids Res.* 17 (1989) 1266.
- [31] Z.A. Sánchez-Quintan, C.Z. Schneider, R.G. Ducati, W.F. de Azevedo Jr., C. Bloch Jr., L.A. Basso, D.S. Santos, *J. Struct. Biol.* 169 (2010) 413–423.
- [32] J.D. de Mendonça, O. Adachi, L.A. Rosado, R.G. Ducati, D.S. Santos, L.A. Basso, *Mol. Biosyst.* 7 (2011) 119–128.
- [33] L.K. Martinelli, R.G. Ducati, L.A. Rosado, A. Breda, B.P. Selbach, D.S. Santos, L.A. Basso, *Mol. Biosyst.* 7 (2011) 1289–1305.
- [34] T.H. Grossman, E.S. Kawasaki, S.R. Punreddy, M.S. Osburne, *Gene* 209 (1998) 95–103.
- [35] F.W. Studier, *Protein Exp. Purif.* 41 (2005) 207–234.
- [36] J.J. Tesmer, T.J. Klem, M.L. Deras, V.J. Davison, J.L. Smith, *Nat. Struct. Biol.* 3 (1996) 74–86.
- [37] W. von der Saal, C.S. Crysler, J.J. Villafranca, *Biochemistry* 24 (1985) 5343–5350.
- [38] X. Zhou, M. Cahoon, P. Rosa, L. Hedstrom, *J. Biol. Chem.* 272 (1997) 21977–21981.
- [39] N.N. Umejiego, C. Li, T. Riera, L. Hedstrom, B. Striepen, *J. Biol. Chem.* 279 (2004) 40320–40327.
- [40] R.G. Ducati, L.A. Basso, D.S. Santos, *Curr. Drug Targets* 8 (2007) 423–435.

- [41] A.D. Vilela, Z.A. Sánchez-Quitian, R.G. Ducati, D.S. Santos, L.A. Basso, *Curr. Med. Chem.* 18 (2011) 1286–1298.
- [42] R. Rodriguez-Suarez, D. Xu, K. Veillette, J. Davison, S. Sillaots, S. Kauffman, W. Hu, J. Bowman, N. Martel, S. Trosok, H. Wang, L. Zhang, L.Y. Huang, Y. Li, F. Rahkhoodaee, T. Ransom, D. Gauvin, C. Douglas, P. Youngman, J. Becker, B. Jiang, T. Roemer, Mechanism-of-action determination of GMP synthase inhibitors and target validation in *Candida albicans* and *Aspergillus fumigatus*, *Chem. Biol.* 14 (2007) 1163–1175.
- [43] L.F. Barker, A.E. Leadman, B. Clagett, *Health Affairs* 30 (2011) 1073–1079.